JTTEE5 15:617-622
DOI: 10.1361/105996306X147207
1059-9630/$19.00 © ASM International

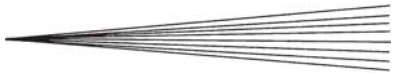

Improving Plasma-Sprayed Yttria-Stabilized Zirconia Coatings for Solid Oxide Fuel Cell Electrolytes

A.A. Syed, Z. Ilhan, J. Arnold, G. Schiller, and H. Weckmann

(Submitted February 23, 2006; in revised form April 20, 2006)

Using a D-optimal design of experiments, the influences of feedstock powder and plasma gases on deposition efficiency, gas tightness, and the electrochemical behavior of vacuum plasma-sprayed yttria-stabilized zirconia for solid oxide fuel cell electrolytes were examined. In-flight particle temperature and velocity, measured by online particle diagnostics, were correlated with plasma and deposit properties. Electrochemical testing of cells was performed to determine the influence of gas tightness and microstructure of electrolyte deposit on cell behavior.

Keywords design of experiments, electrochemical behavior, electrolyte, impedance spectroscopy, in-flight particle diagnostics, ionic conductivity, low-pressure plasma spraying, solid oxide fuel cell, yttria-stabilized zirconia

1. Introduction

Fully yttria-stabilized zirconia (YSZ) is the most widely used electrolyte material in high-temperature solid oxide fuel cells (SOFC) due to its chemical and thermal stability and pure ionic conductivity over a wide range of operating conditions. Pure zirconia exhibits ionic conductivity at temperatures above 2000 °C. Adding divalent or trivalent elements such as yttria in zirconia stabilizes the cubic phase and provides oxygen vacancies. As a result, stabilized cubic zirconia exhibits significant ionic conductivity between 700 and 1000 °C. Because the ionic conductivity is a function of temperature, the initial YSZ-based SOFC were designed to operate at 1000 °C (Ref 1). High operating temperatures, however, impart stringent demands on the materials used in SOFC components such as high-temperature mechanical and chemical stability. Recent research has been directed toward reducing the operation temperature to 800 °C and lower. Using alternative materials such as electrolytes having higher ionic conductivity at lower temperatures is one option. For YSZ-based SOFCs, a reduction in operational temperatures can be achieved by producing thinner electrolytes to compensate for the ohmic losses at lower temperatures. Compared with SOFCs operating at 1000 °C, SOFCs operated at 800 °C can provide similar power output if electrolyte thickness is reduced from 150 to 200 μm (typical for electrolyte-supported cells operating at 1000 °C) down to 10 to 20 μm (Ref 2). However, maintaining acceptable gas tightness becomes an issue for thin electrolytes. The gas tightness of electrolyte is of particular importance in achieving better fuel utilization, and higher open circuit voltage (OCV). Numerous fabrication techniques have been investigated to produce thin gas-tight or hermetic electrolyte layers, with sintering being presently the most extensively used route. Thin electrolytes are produced using tape casting, screen printing, vacuum slip casting, or wet powder spraying followed by heating (Ref 2-4). To ensure gas tightness, sintering of the YSZ has to be done at temperatures above 1400 °C for several hours, resulting in high production costs. Besides, this temperature range limits the cofiring of all cell layers simultaneously, and multicycle sintering has to be performed. Several authors have reported results on electrolyte layers produced via direct vapor phase thin film deposition techniques reviewed by Will et al. (Ref 5). In the last few years, different teams have published results on the fabrication of SOFC layers using thermal spray technologies (Ref 6). Chen et al. (Ref 7) have developed 40 to 70 μm thick electrolyte layers with porosity below 0.5% by triple torch plasma spraying. Fauchais and his coworkers (Ref 8, 9) and researchers at the University of Sherbrooke, Canada, (Ref 10) have presented respectively suspension plasma spraying via direct current (dc) plasma gun and via radiofrequency (RF) and supersonic RF plasma gun as promising alternatives to produce SOFC layers, especially electrolytes. However, no electrochemical results are reported by these researchers. Stöver and his colleagues (Ref 2, 11) have been actively working on the fabrication of SOFC components with plasma spraying, including vacuum plasma spraying (VPS), air plasma spraying by conventional F4 type and new Triplex plasma torches (Sulzer-Metco, Winterthur, Switzerland).

The SOFC group at the German Aerospace Center has been producing complete cells through VPS (Ref 12). Though VPS has many distinct advantages in terms of short fabrication time and simple automation, the quality of cell layers, especially that of electrolytes, needs significant improvement. Due to interla-

This article was originally published in *Building on 100 Years of Success: Proceedings of the 2006 International Thermal Spray Conference* (Seattle, WA), May 15-18, 2006, B.R. Marple, M.M. Hyland, Y.-Ch. Lau, R.S. Lima, and J. Voyer, Ed., ASM International, Materials Park, OH, 2006.

A.A. Syed, Z. Ilhan, J. Arnold, and **G. Schiller,** German Aerospace Center (DLR), Stuttgart, Germany; and **H. Weckmann,** BMW Group, Munich, Germany. Contact e-mail: asif.syed@dlr.de.

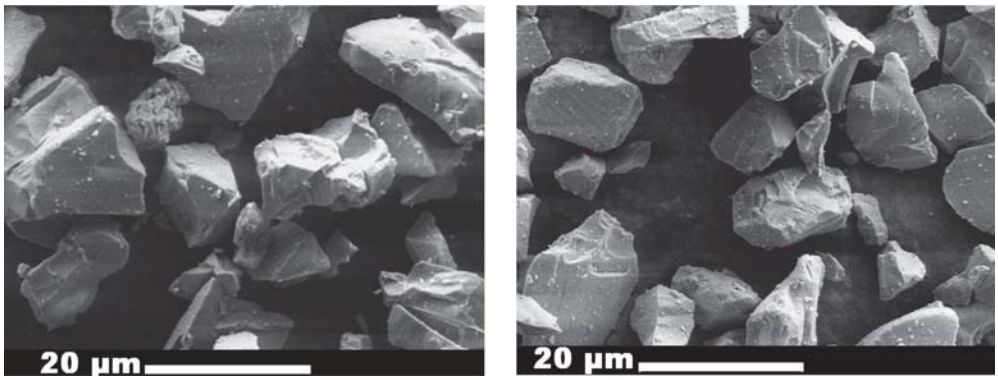

Fig. 1 SEM micrographs of feedstock powders (a) 9.5 mol% YSZ and (b) 8 mol% YSZ

Table 1 Investigated process parameters

Parameter		Minimum	Zero-level	Maximum
Ar, slm	x_1	30	42	54
He, slm	x_2	4	19	34
H_2, slm	x_3	2	5	8

mellar defects and microcracks in electrolyte deposits, the gas tightness and ionic conductivity at high temperature are inferior to those of sintered cells.

In the present work, the influence of plasma-forming gases and feedstock powders on in-flight particle properties and the quality of YSZ deposits was investigated. Instead of using full factorial experiments (requiring 64 runs), the statistical design of experiments (DOE) was opted to limit the number of experimental runs and to get an insight into the interdependence of the studied parameters. The results and developed models were verified using several linear runs.

2. Experimental Procedure

2.1 Feedstock and Plasma Spraying

The feedstock powders were fused and crushed 8 or 9.5 mol% YSZ of a similar particle size range of −22 to +5 µm (Fig. 1) from SulzerMetco and H.C. Starck (Laufenburg, Germany), respectively. The powders were vacuum plasma-sprayed on porous FeCrMnTi substrates (48 mm in diameter, 1 mm in thickness) (Plansee, Reutte, Austria) using an in-house-built, F4-type torch with a convergent-divergent Laval anode. Arc current, standoff distance, and chamber pressure were 600 A, 260 mm, and 8 kPa, respectively. Levels of plasma gases, Ar, He, and H_2, were varied according to a third-degree D-optimal DOE (Table 1, 2). Powder carrier gas flow rate was adjusted to maintain a 3° deviation between the plasma and particle jet axis. The reproducibility of the DOE was checked by repeating twice the whole DOE and four times the zero-level trial (run 1). Using a third-degree D-optimal DOE, an experimental matrix of four variables (levels) and zero level (center point) for each factor can be developed. For instance, 54, 46, 42, 38, and 30 standard liters per minute (slm) for the Ar flow rate correspond to 1, 0.33, 0, −0.33, and −1 levels, respectively, in the matrix system.

Table 2 Trials according to D-optimal DOE (1 to 17) and validation runs (18 and 19)

Run	Ar, slm	He, slm	H_2, slm
1	42	19	5
2	54	34	2
3	30	4	2
4	46	4	8
5	30	14	2
6	38	24	8
7	46	24	6
8	54	34	8
9	30	34	4
10	30	14	8
11	54	4	6
12	46	14	6
13	38	34	2
14	38	4	4
15	54	24	4
16	54	4	2
17	30	34	8
18	35	8	8
19	54	24	2
20	40	0	4

Note: Conventional VPS parameters used at DLR for YSZ are given as run 20.

2.2 Characterization

In-flight particle velocity and temperature were measured by Accuraspray (Tecnar, St.-Bruno, QC, Canada) at a 300 mm standoff distance from the torch nozzle. For shorter distances, radiation from the plasma for several runs limited the precise measurement of particle temperature. Differences of 1.3 to 7.2% and 0.3 to 2.3%, respectively, were estimated in particle temperature and velocity at higher standoff distance for runs in which measurements at 260 mm were feasible. It should be noted that Accuraspray records the average temperature and velocity of particles jet and not those of an individual particle. The deposition efficiency of sprayed powders was calculated as the ratio of coating to sprayed feedstock masses. The former was measured directly as the weight difference of the substrate prior to and after coating. The latter was determined from the powder feed rate and spraying time on the substrate. Gas tightness of electrolytes was evaluated by measuring the leak rate of air through the deposits at room temperature. The pressure difference was introduced across the sample that led to airflow

through the sample. Leak rate values at a 10 kPa pressure difference are given here as reference values. The equipment and technique have been discussed in detail elsewhere (Ref 13). High-temperature ionic conductivity of electrolytes was measured by the 4-point dc method, which has been explained elsewhere (Ref 14). For conductivity measurements, coatings were sprayed on alumina substrates. Conductivity was measured in air as a function of temperature up to 800 °C at a constant heating rate of 5 K/min and as function of time up to 50 h at 800 °C. Observations of fractured and polished samples of deposits were carried out in a LEO 982 (Zeiss, Oberkochen, Germany) scanning electron microscope.

2.3 Electrochemical Testing

Electrochemical testing of SOFCs that were 48 mm in diameter with an effective area of 12.5 cm^2 was performed in a ceramic housing. Following the fabrication of the half-cell composed of a Ni + YSZ anode and YSZ electrolyte by plasma spraying, a 15 μm thick $(La_{0.8}Sr_{0.2})_{0.98}MnO_3$ (LSM) paste was screen printed onto the electrolyte. The cell was placed between the ceramic gas distribution sockets for the anode and the cathode. Coarse platinum meshes on each side of the cell, welded with platinum wires, served as current collector. Two additional platinum wires were used for the voltage measurement between the electrodes. The anode and cathode gas (fuel/oxidizing gas) chambers were isolated by sealing with two gold rings and glass sealant. Sealing was completed by heating the system for 5 h at 900 °C while 0.25 slm of air and Ar + 5vol.% H_2 were fed on the cathode and anode sides, respectively. To have comparable results, cells were tested under similar operating conditions for about 500 h by 200 mA/cm^2 loading at 800 °C with a gas flow of 0.5 slm H_2 + 0.5 slm N_2 at the anode side and 2 slm of air at the cathode side. The continuous loading was interrupted five times for measurements of I-V (current-voltage) behavior and impedance spectroscopy. Details of the test setup and procedure are described elsewhere (Ref 15).

2.4 Regression Analysis

The measured values or responses (leak rate, deposition efficiency, average particle velocity, and average particle temperature) for each run in Table 2 are expressed as polynomials of varied parameters or factors (Ar, He, and H_2). Working with higher-degree polynomials leads to more accurate models. A third-degree D-optimal DOE was therefore used in this work. However, depending on the data distribution of responses, the polynomials were simplified to lower degree. The developed regression equations were validated by using two sets of spray trials within the experimental limits (run 18 and 19). The suitability of models on predicting responses beyond experimental limits is under investigation.

3. Results and Discussion

Polynomial equations obtained after regression analysis for the H.C. Starck 9.5 mol% YSZ are given in Table 3. Except for particle temperature measurements, the predicted and the measured results are in good agreement (Fig. 2), as evidenced by the

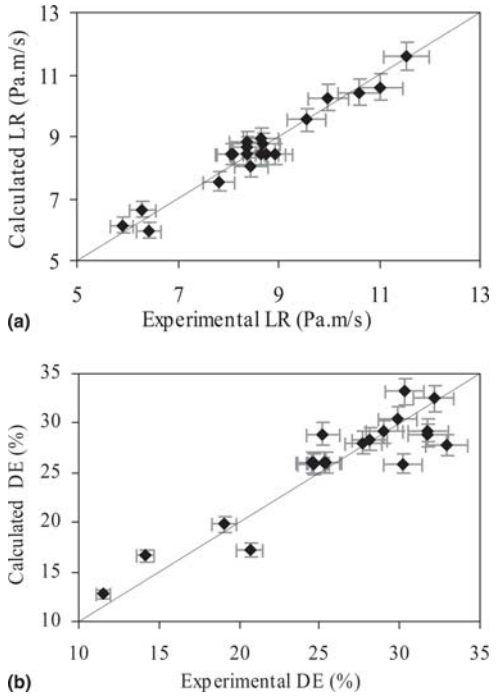

Fig. 2 Correlation between measured data and values calculated from regression analysis for (a) leak rate and (b) deposition efficiency of 9.5 mol% YSZ (−22 to +5 μm).

Table 3 Polynomial equations after regression analysis of results for H.C. Starck 9.5 mol% YSZ (−22 to +5 μm)

Equations	R^2
Leak rate, Pa/m/s	
$y_1 = 15.74 - 0.12x_1 - 0.14x_2 - 0.03x_3 + 1.48 \times 10^{-3}x_2^2$	0.94 (Eq 1)
Deposition efficiency, %	
$y_2 = -0.53 + 0.19x_1 + 0.53x_2 + 3.07x_3 - 0.07x_2x_3$	0.85 (Eq 2)
Mean temperature of particle jet, °C	
$y_3 = 2142.13 + 6.11x_1 + 22.04x_2 + 10.82x_3 - 0.40x_1x_2$	0.56 (Eq 3)
Mean velocity of particle jet, m/s	
$y_4 = 508.19 + 2.32x_1 + 4.47x_2 - 4.69x_3 - 0.07x_1x_2$	0.79 (Eq 4)

relatively high R^2 values shown in Table 3. For the selected gas limits, not much variation in the particle jet temperature was measured. Lower precision for particle temperature measurement is most likely associated with the fact that a deviation in the mean value of up to 12% was recorded. Moreover, particle temperature values were influenced by plasma radiation.

The results obtained for the H.C. Starck 9.5 mol% YSZ (−22 to +5 μm) indicated that the gas leak rate decreases (as the quadratic term in Eq 1 is nonsignificant) and the deposition efficiency improves (as the interaction term in Eq 2 is nonsignificant) with higher flow rates of any of the three gases. However, the primary influence on leak rate is Ar, closely followed by He (8.5% lower than Ar), whereas the effect of H_2 is insignificantly low (96% lower than Ar). On the contrary, H_2 exerts an influence twice as high as Ar and 1.6 times superior to He on the deposition efficiency of 9.5 mol% YSZ. Comparable trends and

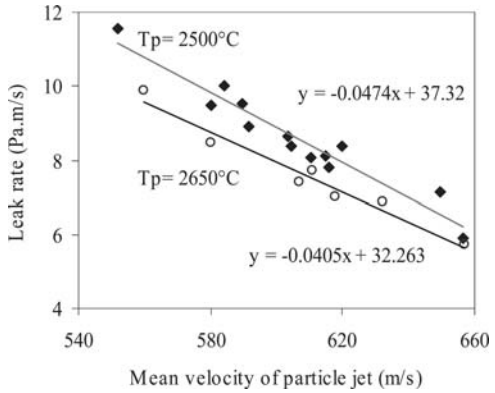

Fig. 3 Leak rate values of 9.5 mol% YSZ deposits as a function of the mean velocity and temperature of a particle jet measured by Accuraspray. Spray parameters, required to obtain desired particle temperature and velocity, were calculated from regression equations.

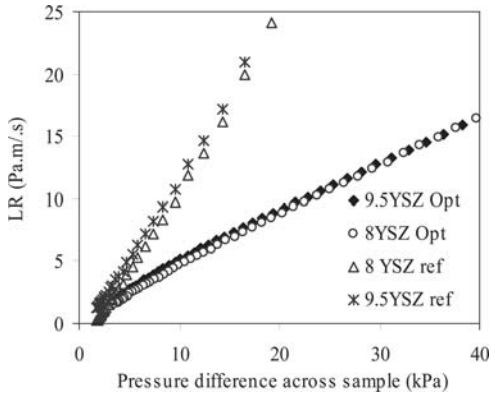

Fig. 4 A mean leak rate of 45 ± 4 μm thick 8 and 9.5 mol% YSZ coatings produced by optimized and reference parameters

Table 4 Spray trials used to evaluate the validity of polynomial equations of Table 3

Spray trial	Ref 18	Ref 19
LR measured, Pa/m/s	9.89 ± 0.74	6.59 ± 0.56
LR from equation, Pa/m/s	10.34	6.72
Relative error, %	−4.5	−2.0
DE measured, %	31.27 ± 1.55	25.51 ± 2.27
DE from equation, %	30.32	28.02
Relative error, %	3.0	−9.9
T_p measured, °C	2518 ± 92	2500 ± 88
T_p from equation, °C	2505	2495
Relative error, %	0.5	0.2
v_p measured, m/s	572 ± 8	635 ± 7
v_p from equation, m/s	567	637
Relative error, %	0.9	−0.3

Note: LR, leak rate; DE, deposition efficiency; T_p, average particle temperature; v_p, average particle velocity

Table 5 Plasma spray parameters optimized after DOE, reference parameters, and corresponding results

Parameters	Optimized		Reference	
Ar, slm	54		40	
He, slm	34		0	
H_2, slm	2		4	
I, A	600		600	
h, MJ/kg	12.1		11.6	
p, kPa	8		8	
Feedstock	9.5% YSZ	8% YSZ	9.5% YSZ	8% YSZ
DE, %	24.3	30.8	20.7	24.7
LR, Pa/m/s	5.95	5.88	11.81	12.01
v_p, m/s	656	…	590	…
T_p, °C	2497	…	2454	…

Note: Standard deviation: LR, ±0.68; DE, ±2.1; v_p, ±11; and T_p, ±80. LR, leak rate; DE, deposition efficiency

regression results were obtained with the SulzerMetco 8 mol% YSZ (−22 to +5 μm). The leak rate values of coatings deposited from both powders were similar, whereas the deposition efficiency for 8 mol% YSZ was 5 to 8% higher. The results of 9.5 mol% YSZ powder are discussed in detail, and a comparison to 8 mol% YSZ is given toward the end.

As the particle velocity is mainly controlled by argon (higher momentum transfer to particles) and helium (higher drag coefficient) (Ref 16), it can be stated from regression analysis that the gas leak rate (dependent on open porosity) can be decreased by using plasma-forming gases leading to higher particle velocity while maintaining sufficient particle melting. Higher thermal conductivity and plasma enthalpy, attained primarily with higher hydrogen and secondarily with helium (Ref 17) can result in increased average particle temperature as well as a higher number of particles reaching melting temperature, which can lead to higher deposition efficiency.

Data on particle velocity and temperature, gathered by Accuraspray using the DOE runs of Table 2, followed the expected trends, as can be seen in the polynomial equations in Table 3. However, the particle velocity was found to decrease with increasing hydrogen content in the plasma. This could be due to the expansion of plasma under soft vacuum conditions with higher hydrogen leading to less efficient plasma-to-particle transfer. The excessive vaporization of particles may occur if the plasma-to-particle thermal conductivity ratio is higher than 0.03 (Ref 18). The resulting vapor cloud limits the plasma-to-particle heat and momentum transfer. These conditions are likely to appear while spraying low-conductivity YSZ in plasma having higher hydrogen molar fraction.

The polynomial equations were verified using experimental trials 18 and 19 of Table 2.

Table 4 compares experimental results to calculated values. A good agreement between the two results can be noticed. Using regression analysis, sets of experiments were later designed to investigate the coating leak rate as a function of particle temperature and velocity, and the results are given in Fig. 3. As predicted from the developed polynomial equations, the leak rate is inversely proportional to particle velocity and temperature; the influence of particle velocity is of prime significance. The optimized and reference spray parameters, after regression analysis of DOE and their experimental validation, are given in Table 5. The pressure difference-dependent leak rate behavior of optimized and reference samples for both powders, presented in Fig. 4 and the SEM micrographs given in Fig. 5, confirm a sig-

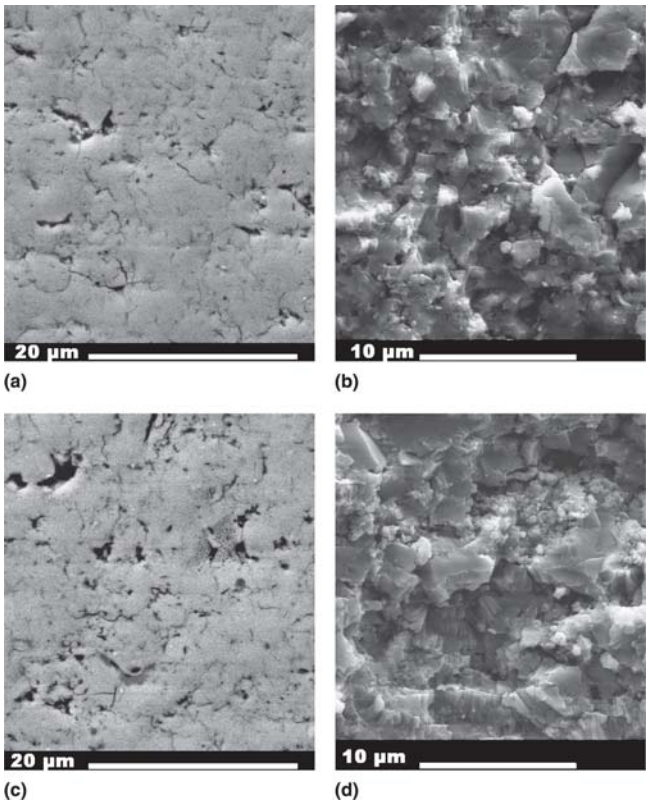

Fig. 5 SEM micrographs of 9.5 mol% YSZ coatings: (a) polished and (b) fractured cross sections of the optimized deposit; (c) polished and (d) fractured cross sections of the reference deposit

nificant improvement in terms of reduced porosity and defects in coatings with optimized parameters leading to lower gas leak rates.

The 9.5 mol% YSZ coatings produced with optimized parameters exhibited 11% higher ionic conductivity at 800 °C compared with coatings produced with reference parameters (Fig. 6). Improved interlamellar contacts can explain the higher conductivity for optimized coatings. However, high-temperature ionic conductivity in ceramics is a complex subject in which the influence of grain boundaries and vacancy distribution needs to be analyzed prior to drawing any conclusions about materials conductivity. A more detailed work on conductivity measurement by impedance spectroscopy is in progress.

During electrochemical testing, the measured OCV for both cells with improved and reference electrolytes remained constant over the total operation time. The cell with the improved electrolyte exhibited an OCV about 50 mV higher compared with the cell with the reference electrolyte (Fig. 7). The measured OCV can be attributed to the gas tightness of either the electrolyte layer or the anode gas sealing. Considering that the sealing applied on both cells was achieved in the same way, it can be stated that the improved electrolyte exhibited better gas tightness at operating temperature, an expected result from the room temperature leak rate measurements of Fig. 4. The measured power density at 0.7 V loading increased within the first 300 h of operation for both cells. The cell with the improved electrolyte presented a power density of 196 mW/cm^2 after

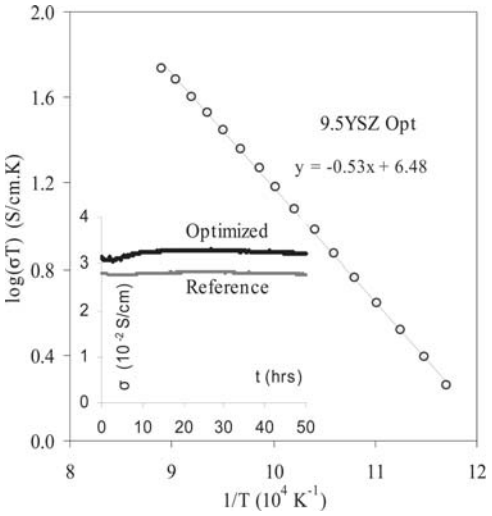

Fig. 6 Ionic conductivity of optimized and reference 9.5 mol% YSZ electrolyte layers

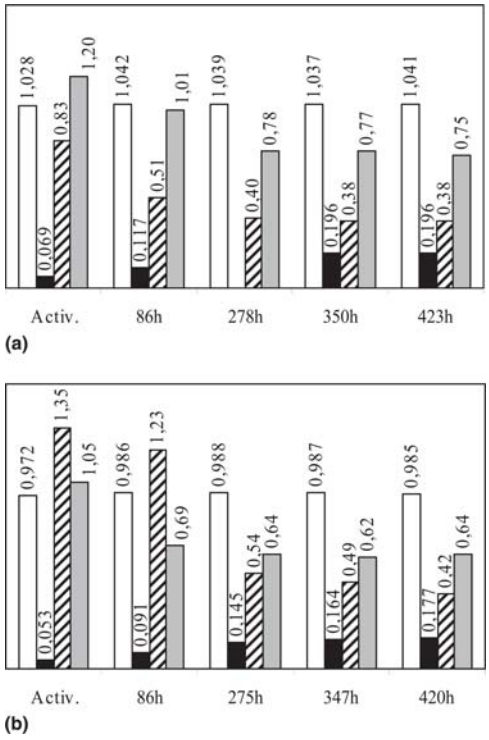

Fig. 7 Electrochemical test results at different intervals of operation time (a and b): white bar, OCV (V); black bar, power density at 0.7 V (W/cm^2); striped bar, ohmic resistance at 200 mA/cm^2 ($\Omega \cdot$ cm^2); gray bar, polarization resistance at 200 mA/cm^2 ($\Omega \cdot$ cm^2) (operating temperature 800 °C; effective cell area 12.57 cm^2; 0.5 to 0.5 slm H_2-N_2, 2 slm Air). (a) Cell with optimized electrolyte. (b) Cell with reference electrolyte

423 h, which was approximately 10% higher than that of the cell with the reference electrolyte. This can be attributed to the higher OCV and better ionic conductivity of the optimized electrolyte because the ohmic resistance was 11% lower. Figure 8

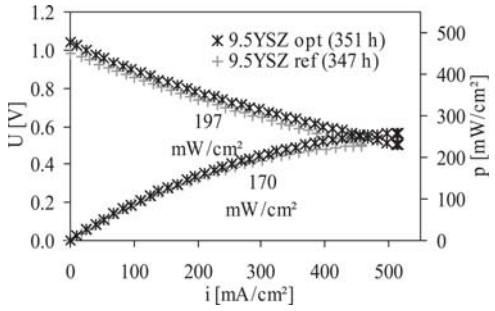

Fig. 8 Current (I) and voltage (V) curves of cells with the optimized and reference electrolytes after about 350 h of operation (operating temperature 800 °C; effective cell area 12.57 cm^2; 0.5 to 0.5 slm H_2-N_2, 2 slm air)

presents the comparison of the I-V curves of both cells. The curves are lying with an offset of about 45 mV. The slopes of the curves, which are attributed to the total cell resistances, are similar. However, the OCV of the cell with the optimized electrolyte was measured to be 51 mV higher than the cell with the reference electrolyte, leading to improved cell operation.

4. Conclusions

Employing a D-optimal DOE, the influence of feedstock powder and plasma-forming gases on in-flight particle properties, deposition efficiency, gas tightness, and electrochemical behavior of vacuum plasma-sprayed YSZ were investigated and described as polynomial equations. The polynomials were validated by several experimental runs by relating calculated and measured values. The higher velocity and temperature of the particle jet resulted in improved gas tightness of YSZ deposits. Particle velocity was shown to have major influence. Deposition efficiency was primarily dependent on particle temperature. With polynomial equations and experimental results, it was demonstrated that the mean particle velocity can be increased primarily by higher flow rates of Ar and He in the plasma, which consequently leads to improved gas tightness. H_2 and He flow rates, governing the particle temperature, had a pronounced effect on deposition efficiency. Compared with the reference 9.5 mol% YSZ electrolyte, deposits produced with optimized parameters exhibited lower porosity, >50% lower leak rates, and 11% higher ionic conductivity at 800 °C. Consequently, an improvement of 50 mV in OCV, 11% in ohmic resistance, and 10% in power density of the SOFCs was measured for the improved electrolyte layers.

Acknowledgments

Financial support for this work by the BMW group, Munich, Germany, is acknowledged, as is the technical assistance of G. Roth and S. Gammert.

References

1. N.Q. Minh and T. Takahashi, *Science and Technology of Ceramics Fuel Cells,* Elsevier, 1995
2. F. Tietz, H.-P. Buchkremer, and D. Stöver, Components for Solid Oxide Fuel Cells, *Solid State Ionics,* 2002, **152-153,** p 373-381
3. J. Liu, W. Liu, L. Pei, L. Jia, L. He, and W. Su, Study on the Properties of YSZ Electrolyte Made by Plaster Casting Method and the Applications in Solid Oxide Fuel Cells, *Solid State Ionics,* 1999, **118,** p 67-72
4. Y. Zhang, J. Gao, D. Peng, M. Guangyao, and X. Liu, Dip-Coating Thin Yttria-Stabilised Zirconia Films for Solid Oxide Fuel Cell Applications, *Ceram. Int.,* 2004, **30,** p 1049-1053
5. J. Will, A. Mitterdorfer, C. Kleinlogel, D. Perednis, and L.J. Gauckler, Fabrication of Thin Electrolytes for Second Generation Solid Oxide Fuel Cells, *Solid State Ionics,* 2000, **131,** p 79-96
6. F. Gitzhofer, M.I. Boulos, J. Heberlein, R. Henne, H. Ishigaki, and T. Yoshida, Integrated Fabrication Processes for Solid-Oxide Fuel Cells Using Thermal Plasma Spray Technology, *MRS Bull.,* 2000, **25**(7), p 38-42
7. H.C. Chen, J. Heberlein, and T. Yoshida, *13th International Symposium on Plasma Chemistry,* C.K. Wu, Ed. IUPAC Subcommittee on Plasma Chemistry, Beijing, China, 1997, p 320-326
8. P. Fauchais, V. Rat, C. Delbos, J.F. Coudert, T. Chartier, and L. Bianchi, Understanding of d.c. Suspension Plasma Spraying of Finely Structured Coatings for SOFC, *IEEE Trans. Plasma Sci.,* 2005, **33**(2), p 920-930
9. C. Delbos, V. Rat, C. Bonhomme, J. Fazilleau, J.F. Coudert, and P. Fauchais, Influence of Powder Size Distributions on Microstuctural Features of Finely Structured Plasma Sprayed Coatings, *High Temp. Mater. Proc.,* 2004, **8,** p 397-406
10. F. Gitzhofer, M.E. Bonneau, and M.I. Boulos, Double Doped Ceria Electrolyte Synthesized by Solution Plasma Spraying with Induction Plasma Technology, *Thermal Spray 2001: New Surfaces for a New Millennium,* C.C. Berndt, K.A. Khor, E.F. Lugscheider, Ed., May 28-30, 2001 (Singapore), ASM International, 2001, p 61-68
11. D. Stöver, D. Hathiramani, R. Vaßen, and R.J. Damani, Plasma-Sprayed Components for SOFC Applications, *2 Rencontre Internationales sur la Projection Thermique,* L. Pawlowski, Ed., December 1-2, 2005 (Lille, France) 2005, p 171-177
12. G. Schiller, R. Henne, M. Lang, R. Ruckdäschel, and S. Schaper, Development of Vacuum Plasma Sprayed Thin-Film SOFC for Reduced Operating Temperature, *Fuel Cells Bull.,* 2000, **21,** p 7-12
13. S.E. Pohl, "Fabrication and Leak Test of Plasma-Sprayed YSZ Electrolytes and Cells for SOFC," Masters thesis, DLR, University of Hanover, 2001 (in German)
14. T. Kholwad, "Electrical and Electrochemical Characterization of Vacuum Plasma Sprayed Functional Layers in Solid Oxide Fuel Cells," Masters thesis, DLR, BMW, University of Applied Sciences Offenburg, 2005
15. T. Franco, M. Lang, G. Schiller, P. Szabo, W. Glatz, and G. Kunschert, Powder Metallurgical High Performance Materials for Substrates-Supported IT-SOFCs, *6th European SOFC Forum,* M. Mogensen, Ed., European Fuel Cell Forum, 2004, p 209-217
16. B. Dussoubs, "3D Modelling of Plasma Spray Processing: Influence of Particle Injection and Spray Parameters on the Treatment and Distribution of Particles in the Jet," Ph.D. thesis, University of Limoges, 1998 (in French)
17. M.I. Boulos, P. Fauchais, and E. Pfender, *Thermal Plasmas: Fundamentals and Applications,* Vol 1, Plenum Press, New York, 1994
18. P. Fauchais and A. Vardelle, Heat, Mass and Momentum Transfer in Coating Formation by Plasma Spraying, *Int. J. Thermal Sci.,* 2000, **39** (9-11), p 852-870